

## **Model-Based Fault Detection for Hydraulic Servoproportional Valves**

José Roberto Branco Ramos Filho\* and Victor Juliano De Negri

LASHIP, Mechanical Engineering Department, Federal University of Santa Catarina, Florianópolis, SC, Brazil

E-mail: robertobrancofilho@gmail.com, victor.de.negri@ufsc.br

\*Institute of Engineering and Geosciences, Universidade Federal do Oeste do Pará, Santarém, Pará, Brazil

### **Abstract**

This paper presents a mathematical model for online fault detection on single solenoid servoproportional spool valves. The most common failures as well as its effects on the valve behavior are studied and took into account for the model representation. Servoproportional valves are used in industry, aerospace, and military fields. Some of these uses are critical-mission, where the valve must not fail without previous warning to prevent or mitigate financial losses, equipment damage, and risk to personnel. Even in less demanding applications, it is very useful to be able to quickly locate a failure in the hydraulic circuit, which is a task that may demand up to 80% of the time used in corrective maintenance. Total failure can readily be detected using the signals available on the valve electronics. However, since the spool positioning is on closed loop on these valves, incipient failures that can be overcome by the controllers cannot be easily detected. In this paper, an experimentally validated analytical model is used as a reference model such that the solenoid actual current can be compared with the theoretical current. Since the valve hysteresis is considered, the model calculates maximum and minimum current values that correspond to an undamaged valve. Experimental results with a standard valve and a damaged valve show the effectiveness of the model for fault detection.

**Keywords:** hydraulics, proportional valves, fault detection.

### **1 Introduction**

Electrically modulated hydraulic control valves [1], particularly servoproportional spool valves, are used in several applications in industry, aerospace, and military fields. Some of these applications are critical-mission, where the valve must not fail without previous warning to prevent or mitigate financial losses, equipment damage, and risk to personnel. Even in less demanding applications, it is very useful to help quickly locating a failure in the hydraulic circuit, which is a task that may demand up to 80% of the time used in corrective maintenance. Also, a valve who has not lost its function, but is not operating at its best may affect the entire hydraulic system performance, making it hard for engineers to locate and solve the problem [2].

A fault detection process isolates the source of a system malfunction through the gathering and the analysis of information about the current state of the system obtained through measurement, testing and other sources of information, such as the user [3]. Since the detection is usually performed in embedded systems with other functions, such as control, the fault detection process should be as simple as possible. The attempt to detect all possible failures would make the process unnecessarily complex and would increase its response time. That is why embedded fault detection systems are made to quickly detect the most common faults. On the other hand, running complex tests periodically would not compromise the system safety [4].

The evaluation of the acquired data from the system is important to the decision making process and it can be done using techniques such as artificial intelligence, behavior or failure models, signal analysis, process history, statistical methods and others [3], [5]. The model based approach requires extensive effort during the development phase, and is computer intensive when used on-line, but is adaptable to other similar equipment through parameter and model adjustments. The model development process also adds knowledge over the system under study [5]. For these reasons, the model approach has been chosen by the authors to generate the necessary information for decision making.

### **2 Common failures in spool valves**

Electrically modulated hydraulic control valves should have a service life of several million cycles when operated with adequate filtered fluid within the boundaries of its nominal specifications. However, its service life is greatly influenced by operational conditions such as the environment where it is installed, fluid contamination, the use of dither, pressure and voltage spikes, etc.

Among the most common failures are the ones caused by contaminated fluid and degraded components due to excessive wear [2]. In order to gain some knowledge on how these failures affect the valve and what should be monitored to detect such a situation, the most common faults are discussed below [2], [6].

## 2.1 Solenoid fault

After the solenoid reaches the magnetic saturation current level, additional current through the solenoid will only cause it to generate heat. This increases its impedance and therefore decreases the current through the solenoid for a certain voltage. This also reduces its ability to generate mechanical force. In extreme cases the core may fracture or the coil inductance may be permanently altered. When the solenoid burns it becomes an open circuit, and no current goes through no matter the voltage applied. This causes the valve not to respond to the command signal, and therefore no spool movement will be possible.

## 2.2 Spring fault

A broken or fatigued spring may cause the spool to drift, since it is subject only to both the solenoid and to the steady-state flow forces. A valve with a broken spring is not able to comply with the command signal, even though the solenoid is working properly.

## 2.3 Fluid fault

According to [7], up to 75% of the failures in hydraulic systems are caused by contamination generated or added to the system. The undesirable effects include frequent component replacement, loss of movement repeatability, parameter alteration, fluid degradation and others. Among the most common contaminants are those presented below.

### 2.3.1 Solid particles

The gap between the spool lands and the sleeve of control valves ranges from 1 to 25  $\mu\text{m}$  according to the valve size and design. Particles around that size can silt or become wedged in the spool or sleeve, leading to erratic movements, jamming, and permanent damage to lands, orifices and sleeve [8]. Contaminants such as sand, metal particles, polish compound, and other residues can cause wear and premature failure, making this kind of contaminant one of the critical factors to affect the service life and the reliability of hydraulic systems [9], [10], [11]. These contaminants may come from the external environment or may come from the wear of components of the system.

How long it will take for this to occur depends on the amount and size of particles, and on the pressure differential, varying from a few seconds to a few hours if the valve is centered [9], [8]. Particles ranging from 5  $\mu\text{m}$  to 40  $\mu\text{m}$  may quickly jam a valve, and occurrences even during the commissioning of the machine have been reported [8].

In the long run, particle contamination may cause increased friction between the spool and the sleeve, increasing hysteresis, scratching the spool surface and eroding edges, increasing flow and non-linear behavior in the center position. This state demands more from the solenoid, who has to operate at higher current levels to move the spool, increasing both threshold and flow gains, and decreasing pressure gains. When the valve is extremely damaged its responses may become slower, unstable or fail completely

due to the clogging of orifices or to the failure of the solenoid [9], [8].

### 2.3.2 Water

Water may be dissolved in the fluid up to the saturation point, and then the excess presents as a second phase (free water) or an emulsion. Water contamination can lead to failures such as corrosion of surfaces, accelerated abrasive wear, metal fatigue, and increased friction due to viscosity loss among others. These effects will lead to the increase of the force necessary to move the spool. Even greater complications may occur when the temperature decreases, since the fluid holds less dissolved water under these conditions, and when the freezing point is reached, the formation of ice crystals may affect the system functions [12].

### 2.3.3 Air

The air may be dissolved or free in the hydraulic fluid. Though it causes less trouble when dissolved, it may cause jamming, erratic functioning and other undesirable effects when it is trapped inside a valve [13]. The air may come from leaks in the system, from maintenance interventions, or from fluid turbulence in the reservoir.

### 2.3.4 Varnish and slug

Varnish and slug are generated by the degrading of the hydraulic fluid, which may happen as a result of natural aging, overheating, or the presence of contaminants such as water, air, solid particles, among others. It may be dissolved or free in the fluid. The fluid capacity to hold them dissolved depends greatly on the fluid temperature [9]. The varnish may accumulate in low flow and low temperature areas of the system, while areas with a high flow or high temperature are not affected. This kind of contaminant affects particularly valves that are not used for a certain period of time, like the ones used in emergency systems or during the cold start of a machine with degraded fluid [14].

These residues may clog orifices and grooves making the valve sluggish. In such a state the valve experiences jamming and performance loss. Also, solid particles may accumulate on the sticky surface, creating an abrasive surface that accelerates the wear of the moving parts of the system [14].

## 2.4 Other factors

Other factors may cause problems, such as pressure spikes, electrical surges, fatigue and manufacturing defects. Pressure spikes and electrical surges may be generated by accidents or design problems. When pressure spikes occur, damage to internal components, valve manifold an leaks may affect the valve, causing alterations in its behavior. Electrical surges may damage the electronic components of a servoproportional valve, rendering it useless. Fatigue and manufacturing defects such as problems in the valves surfaces, component alignment, geometry of chambers and drains, or even broken mechanical components, who may be

noticed on valve commissioning of after a period of operation, will affect greatly the valve behavior.

As seen above, in electrically modulated hydraulic control spool valves, the most common failures may cause the increase of friction between the spool and the sleeve due to wear, abrasion, varnish and particle accumulation, that end up altering the valve frictional characteristics [15]. Those may increase the stick and slip phenomenon, where the spool moves and stops several times during its trajectory, causing the actuator to move irregularly, and may even jam the valve spool. Some failures, such as damaged electronic components or broken mechanical components may affect the valve ability to control the forces on the spool. For that reason it is important to have some estimate of the forces that would normally be present. Since the force applied on the valve by the solenoid is fairly proportional to the current through its coil, an estimate of normal current levels can be used for comparison with the actual current levels through the solenoid to detect faults. Knowing the current that should be applied at the solenoid at each spool position at a certain operating condition may help the operator or monitoring system to realize when the valve is not working properly even before the fault could be noticed through other of the valve signals, such as spool position.

### 3 Servoproportional valve modeling

#### 3.1 Force and current equations

From the previous section one can realize that the magnitude of the forces involved in the spool movement is affected in most of the failures mentioned in the researched literature. Servoproportional valves are built with solenoids stronger than the needs to overcome the valve internal forces in order to be able to move even in the presence of certain contaminants or at higher pressure differentials. This is why the difference between the current levels of a healthy valve are so different from the levels of a contaminated or damaged valve, since the controller uses the extra power when it is not able to move the spool. Therefore, a model to estimate the internal forces through the magnitude of the current that should be applied at each spool position at certain operation conditions was developed [16]. In order to do so, a closer look at the forces involved in the spool movement is required.

The axial force required to move the spool is a consequence of the necessary forces to accelerate the spool and anything else that moves with it, to overcome friction, and the forces due to the flow through the valve, also called flow induced forces or Bernoulli forces [9]. There is also the force necessary to overcome springs used to center or return the spool valve.

Regarding the flow forces, the most significant is the steady-state flow force that is related to the variation of the quantity of motion of the fluid in the valve chambers (fig. 1). The jet angle is typically at around  $69^\circ$  from the center axis of the spool if the radial clearance between the spool and the sleeve is neglected [9]. Therefore, the resulting force has a lateral component that pushes the spool against the sleeve or

body of the valve, and an axial component that tends to shut the valve closed. Commonly the ports of the valve are located symmetrically around the spool, leading the components of the lateral force to compensate each other. However, the axial forces are not compensated except the valve has a flow force compensation design.

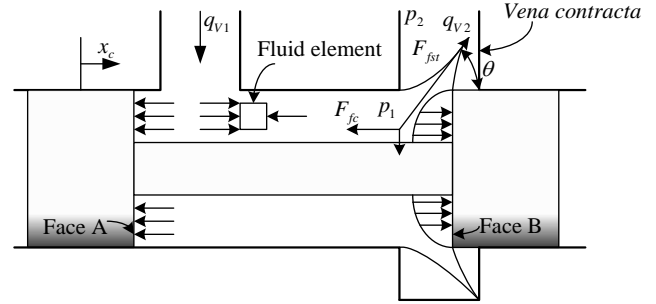


Figure 1: Flow forces on a spool valve due to flow leaving a valve chamber [9].

The steady-state flow force can be expressed for each valve chamber as [9], [17], [18]

$$F_{fst} = \frac{\rho \cdot q_v^2}{cc \cdot A_0} \cdot \cos \theta \quad (1)$$

where:

$F_{fst}$  is the steady-state flow force in axial direction [N];

$\rho$  is the fluid mass density [kg/m<sup>3</sup>];

$q_v$  is the volumetric flow rate through the valve [m<sup>3</sup>/s];

$A_0$  is the metering orifice area [m<sup>2</sup>];

$\theta$  is the jet angle at the *vena contracta* [no dimension].

$cc$  is the contraction coefficient that relates the area at the metering office to the area at the *vena contracta* [no dimension].

This force is applied over the fluid. Consequently, the reaction force on the spool ( $F_{fc}$ ) has the same module but inverse signal.

Using the valve flow coefficient defined in [19], the flow rate can be expressed by [20]

$$q_v = Kv \cdot \frac{x_c}{x_{cn}} \cdot \sqrt{(p_1 - p_2)} \quad (2)$$

where:

$x_c$  is the valve spool displacement [m];

$x_{cn}$  is the nominal spool displacement, at which the  $Kv$  is obtained [m];

$Kv$  is the valve flow coefficient [m<sup>3</sup>/s.√Pa];

$p_1$  is the inlet pressure [Pa];

$p_2$  is the outlet pressure [Pa].

Since that the flow coefficient can be expressed by [20]

$$K_v = cd \cdot A_{0n} \cdot \sqrt{\frac{2}{\rho}} \quad (3)$$

where:

$A_{0n}$  is the nominal metering orifice area [m<sup>2</sup>];

$cd = cv \cdot cc$  is the discharge coefficient [no dimension];

$cv \approx 1$  is the velocity coefficient [no dimension];

the reaction force  $F_{fc}$  can be written combining eq. (1), eq. (2), and eq. (3):

$$F_{fc} = \frac{K_v \cdot x_c \cdot \sqrt{2 \cdot \rho \cdot (p_1 - p_2)} \cdot \cos \theta}{x_{cn}} \quad (4)$$

The force above contributes significantly to the force required to stroke the valve spool [9]. One can notice that the reaction force ( $F_{fc}$ ) is proportional to the spool displacement and therefore it can be represented by  $F_{fc} = K_{esc} \cdot x_c$  where  $K_{esc}$  [N/m] is a variable stiffness.

Therefore, the necessary force to move the valve spool can be expressed as

$$F_c = m_e \cdot \ddot{x}_c + B_e \cdot \dot{x}_c + K_{me} \cdot x_c \quad (5)$$

where:

$F_c$  is the force necessary to move the valve spool [N];

$m_e$  is the equivalent moving mass [kg];

$B_e$  is the equivalent viscous friction coefficient [N.s/m];

$K_{me} = K_m + K_{esc}$  is the effective spring rate [N/m];

$K_m$  is the spring rate [N/m].

The inertial force is related to the effective moving mass that consist the mass of the valve moving parts plus fluid contained in the valve chambers and drain ports at the spool ends. The dampening forces are a consequence of the transient flow forces related to flow acceleration and the viscous friction forces caused by the fluid adjacent to the valve moving parts. These forces are in general considerably smaller than the spring and steady-state flow forces and can be neglected in the model for simplicity sake. Their effect, however, is important, since they limit the valve performance and response time and may demand the solenoid maximum available force during the initial acceleration of the spool when changing the area of the

metering orifices. For this reason measures must be taken in the fault detection process to avoid false detections [16].

This yields a much simpler, easier to calculate model, allowing a reduced processing time for on-line fault detection. In a solenoid valve all these forces must be overcome by the solenoid(s). Since the force generated by the solenoid(s) can be described in a simplified way by [18]

$$F_s = K_{Fi} \cdot i_s \quad (6)$$

where:

$F_s$  is the force produced by the solenoid [N];

$K_{Fi}$  is the solenoid force - current coefficient [N/A]

$i_s$  is the current on the solenoid [A].

Substituting eq. (6) in eq. (5) and considering steady-state conditions one obtains:

$$i_s = \frac{K_{me}}{K_{Fi}} \cdot x_c \quad (7)$$

### 3.2 Model applied to the studied valve

The Hydrus, HR01 servoproportional single solenoid valve is a prototype valve designed at LASHIP/UFSC. Since there is no failure field data and the magnitude of the internal forces at such operational conditions, the choice for the model based approach was reinforced, since it could be based on the in lab valve behavior [16].

Being a single solenoid valve, the HDR01 has only one spring, as seen in Fig. 2. This spring counteracts the solenoid and to this force the steady-state flow force is added. At the beginning of the solenoid displacement, when the current and the force yielded by the solenoid is zero, the valve port A is fully open and connected to the supply port, while the port B is connected to the return port. Following the center position, where all ports are closed, the valve connects the port B and the supply port at the same time it connects the port A and the return port. Since the steady-state flow forces tend to close the valve, while the port A is connected to the supply port the steady-state flow forces help the solenoid against the spring. After the center position, the steady-state flow forces act against the solenoid along with the spring.

As it typically occurs, the proportional solenoid has non-linear regions at the beginning and at the end of its displacement. These regions were avoided to make the valve proportional, but the non linearity offsets the force curve from zero, since the solenoid only starts generating force after a certain current is applied. Also, the solenoid presents hysteresis on its force versus current relation, as a result of the remanence phenomenon, which is the residual magnetization of a ferromagnetic material in the absence of external magnetic fields. Therefore it is necessary to add a linear coefficient to eq. (7) in order to compensate the force offset. This coefficient has two values in order to account

for the hysteresis of the solenoid, delimiting the maximum and minimum force yielded for a given current level.

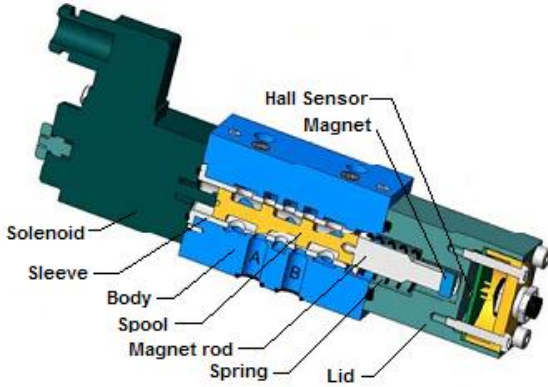


Figure 2: HR01 servoproportional valve

The force actually generated by the solenoid at a certain current will depend on its previous movements and on which way it is moving. Hence

$$F_s = K_{Fi} \cdot i_s + b_s \quad (8)$$

where:

$b_s$  is the solenoid force x current curve linear coefficient [N].

Therefore, associating eq. (4), eq. (7) and eq. (8), regarding the characteristics of the valve one has, for  $x_{c\min} \leq x_c \leq x_{c\max}$ ,

$$i_s = \left[ \frac{\sqrt{2 \cdot \rho \cdot Kv \cdot \cos \theta} \cdot \Delta p}{x_{cn} \cdot K_{Fi}} + \frac{K_m}{K_{Fi}} \right] \cdot x_c + \left[ \frac{-\sqrt{2 \cdot \rho \cdot Kv \cdot \cos \theta} \cdot x_{c0} \cdot \Delta p}{x_{cn} \cdot K_{Fi}} + \frac{K_m \cdot x_{m0} - b_s}{K_{Fi}} \right] \quad (9)$$

where:

$x_{c0}$  is the spool center position [m];

$x_{c\min}$  is the minimum spool displacement for which the valve is linear [m];

$x_{c\max}$  is the maximum spool displacement for which the valve is linear [m].

$x_{m0}$  is the valve spring initial displacement [m];

Equation (9) can be rearranged into:

$$i_s = a_i \cdot x_c + b_i \quad (10)$$

where:

$a_i$  is the angular coefficient of the current estimate model [A/m];

$b_i$  is the linear coefficient of the current estimate model [A].

These coefficients can be expressed as

$$a_i = \left[ \frac{\sqrt{2 \cdot \rho \cdot Kv \cdot \cos \theta}}{x_{cn} \cdot K_{Fi}} \right] \cdot \Delta p + \left[ \frac{K_m}{K_{Fi}} \right] \quad (11)$$

and

$$b_i = \left[ \frac{-\sqrt{2 \cdot \rho \cdot Kv \cdot \cos \theta} \cdot x_{c0}}{x_{cn} \cdot K_{Fi}} \right] \cdot \Delta p + \left[ \frac{K_m \cdot x_{m0} - b_s}{K_{Fi}} \right] \quad (12)$$

Both eq. (11) and eq. (12), however, can be further divided in angular and linear coefficients regarding  $\Delta p$  forming the equations below

$$a_i = a_{a_i} \cdot \Delta p + b_{a_i} \quad (13)$$

$$b_i = a_{b_i} \cdot \Delta p + b_{b_i} \quad (14)$$

where:

$a_{a_i}$  is the angular coefficient that adjusts  $a_i$  to the pressure drop on the valve [A/m.Pa];

$b_{a_i}$  is the linear coefficient that adjusts  $a_i$  to the pressure drop on the valve [A/m];

$a_{b_i}$  is the angular coefficient that adjusts  $b_i$  to the pressure drop on the valve [A/Pa];

$b_{b_i}$  is the linear coefficient that adjusts  $b_i$  to the pressure drop on the valve [A].

From eq. (10), eq. (13), and eq. (14) a Simulink block diagram has been designed as shown in fig. 3. This block diagram estimates the maximum and the minimum current at the solenoid at a certain spool position for a given pressure drop on the valve. It is supposed to estimate the steady-state current, but since the effective spring forces are considerable, it can be used too to estimate with a reasonable margin of error the transient current that occurs when the solenoid and valve are accelerating, since the estimates change as the spool moves. Under steady-state conditions the current value is to be around the range delimited by the two estimated limits, or slightly above or below if hunting occurs due to the static friction of the spool, which is a non-linear characteristic not accounted for in the model.

The model expressed in Fig. 3 is fit for a symmetrical proportional valve. For an asymmetrical valve, two of these block diagrams should be used in order to change the  $Kv$  value as the valve changes the flow direction.

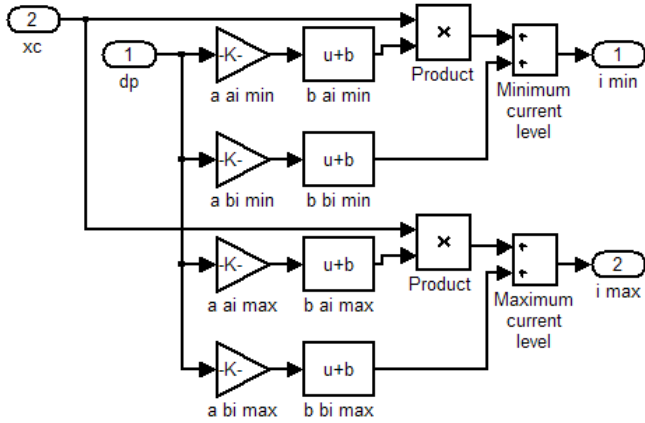


Figure 3: Solenoid current estimation model

Signals obtained from sensors that measure spool position, supply pressure, return pressure, chamber A pressure, and chamber B pressure are used by the model to output two current estimates, the maximum and the minimum current levels expected for that spool position at those operating conditions. Running in parallel with the valve, as shown in fig. 4, the model generates real time estimates that can be compared to current on the valve solenoid to detect discrepancies, and therefore, potential faults. Depending on the characteristics of those discrepancies, a certain type of fault is more likely to be happening, information that is valuable for diagnosis and to narrow down maintenance actions to solve the problem.

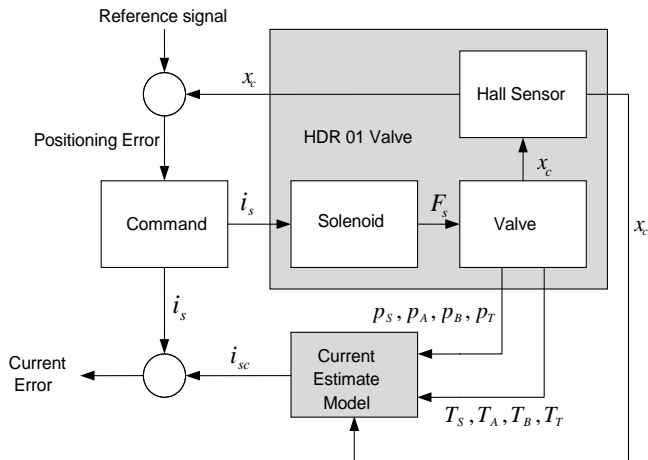


Figure 4: Current on the solenoid estimate model running in parallel with the actual valve

### 3.3 Experimental results

Firstly, experiments were made to check the modeling hypothesis and evaluate the need for models that account for temperature changes. In fig. 5a the valve behavior under different supply pressure levels can be seen, showing that current changes relatively linearly with spool displacement, and the rate of this change varies with the supply pressure on the valve. This is a consequence of the changing of valve flow rate with pressure, as shown in fig. 5b. Notice that flow rates below to 2.5 l/min are out of the measuring range of the flow transducer used in these experiments, and the sudden drop in the flow rate close to the valve center does

not occur. During these experiments the ports A and B were interconnected and the temperature controlled at  $40 \pm 2^\circ\text{C}$ .

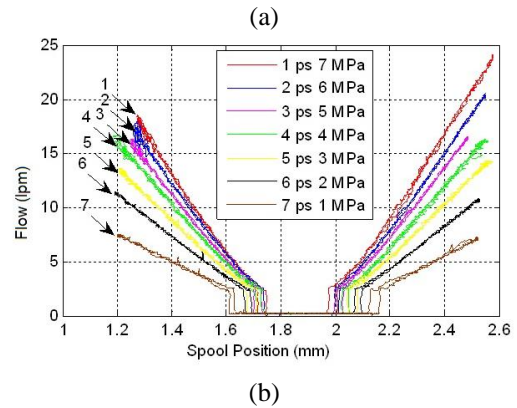
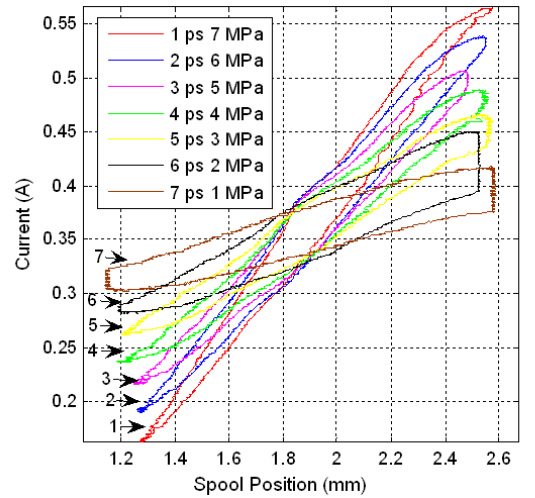


Figure 5: Results with different  $p_s$  at  $40^\circ\text{C}$ : (a) Current on the solenoid  $x$  spool position; (b) Flow rate  $x$  spool position

Figure 6a shows that flow rate does not change within the temperature range such that there is a small variation in the current levels necessary to move the spool (fig. 6b). For greater temperature changes further compensations may be needed on the model. In figures 5a and 6b the effect of hysteresis and threshold can be noted, since two different current levels are seen for the same spool position, depending on the spool moving direction.

Based on these results, the temperature effect was not included in the model. However, a model using temperature sensors to estimate the pressure drop between the supply port and port A (or B, depending on the flow direction) and the other working port and the return port was developed to replace the pressure measurements. That would make the hardware necessary to feed the model cheaper. However, the temperature sensors readings were too slow to keep up with the spools movements, and that could lead to false detections.

The model was validated using both parameters extracted from the product catalog and experimental parameters, extracted from fig. 5a. Good results were achieved with both approaches however the use of experimental parameters resulted in a more accurate current estimation, as expected.

Merritt [9] discusses about the uncertainty of the flow force theoretical models, especially when the spool is close to the center, due to the changes in the jet angle at the *vena contracta* and other simplifications as the orifice geometry. Experimental parameters can reduce the influence of these simplifications and variations that occur from valve to valve. However, the model with theoretical values is still good enough for estimate due to the considerable differences in current observed when the valve is contaminated or worn.

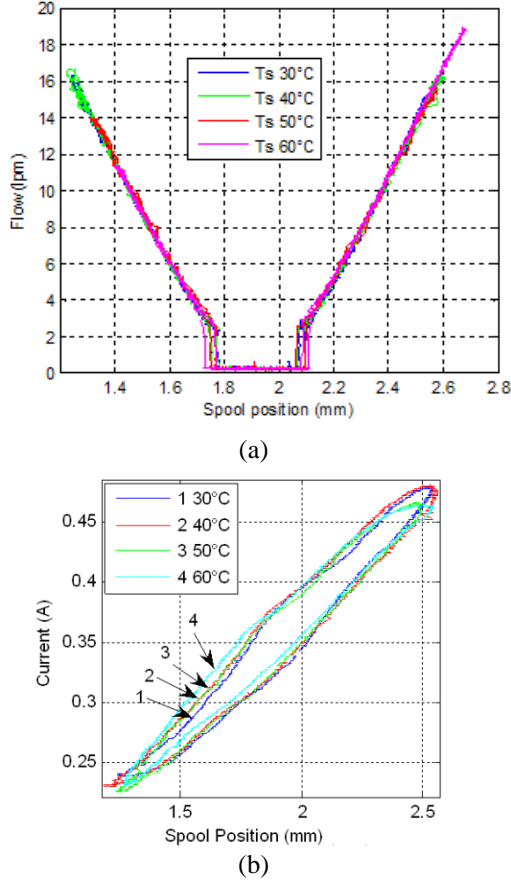


Figure 6: Results with different  $T_S$  at  $p_s = 4$  MPa: (a) Flow rate  $\times$  spool position; (b) Current  $\times$  spool position.

The experiments were carried out on a test rig according to recommendations from ISO 10770-1 [1]. Valve port A was connected to port B and supply temperature  $T_S$  adjusted from 30°C to 60°C. Supply pressure  $p_s$  ranged from 3 to 5 MPa. Step inputs ranging from 1.32 to 2.43 mm and sinusoidal inputs from 1.32 to 2.43 mm with periods ranging from 1 to 20 s were used [16]. Figure 7a shows the solenoid current  $i_s$  response for a position step input from 1.85 to 1.635 mm compared with the minimum and maximum current estimates using experimental values and catalog/theoretical values to obtain the coefficients  $a_{a_i}$ ,  $b_{a_i}$ ,  $a_{b_i}$ , and  $b_{b_i}$ .

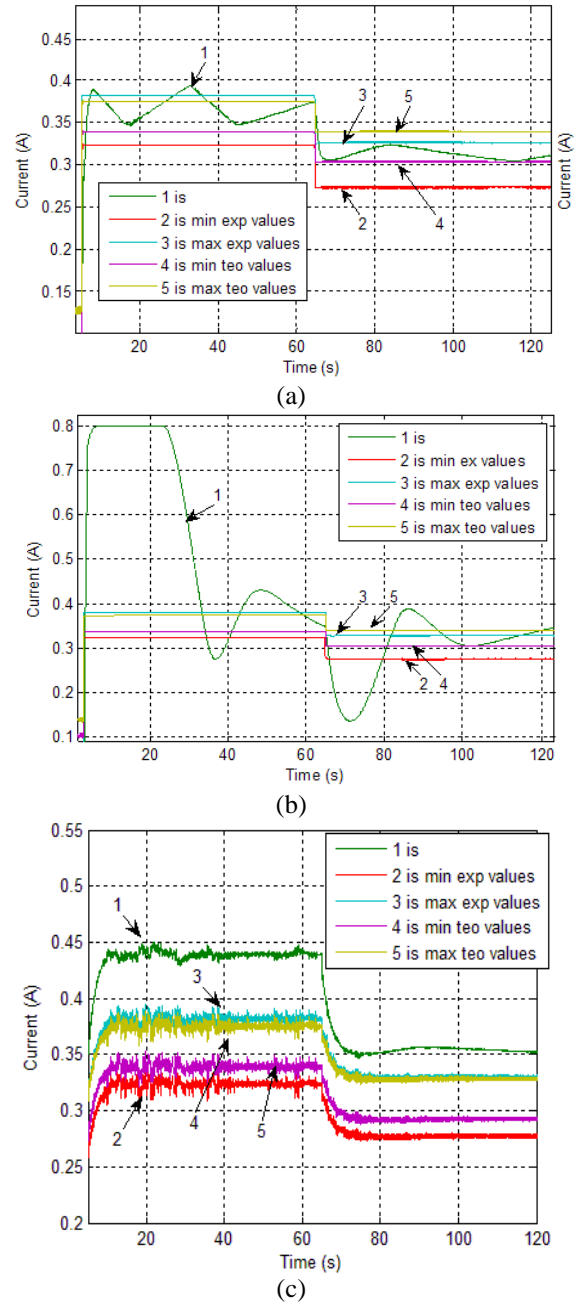


Figure 7: Current for step inputs of 1.85mm and 1.635 mm at  $p_s = 4$  MPa and  $T_S = 40^\circ\text{C}$ : (a) healthy valve (b) degraded valve (c) contaminated valve

The greatest difference between the estimated and the actual current for a healthy valve was observed during the first 10% of the settling time after a step input. Since the estimate is based on a steady state model, the difference between the estimated and the actual current is maximum when the spool is being accelerated or decelerated. During steady-state conditions the current remained within the boundaries of the estimates for most of the time, except when hunting occurred. Here some error was noticed due to the spool static friction, which forced the controller to raise the current to move the spool while the spool remained still.

The sinusoidal response is presented in fig. 8a where the error corresponds to the percentage difference between the

actual and estimated current. When considering the minimum estimate value, the error must be positive or very close to zero which means that the actual current is higher than the minimal estimated value. In the same way, for maximum estimate currents the error must be negative or very close to zero for a healthy valve. It is not accomplished when the movement direction of the spool changes since that the dynamic effects are not computed by the model.

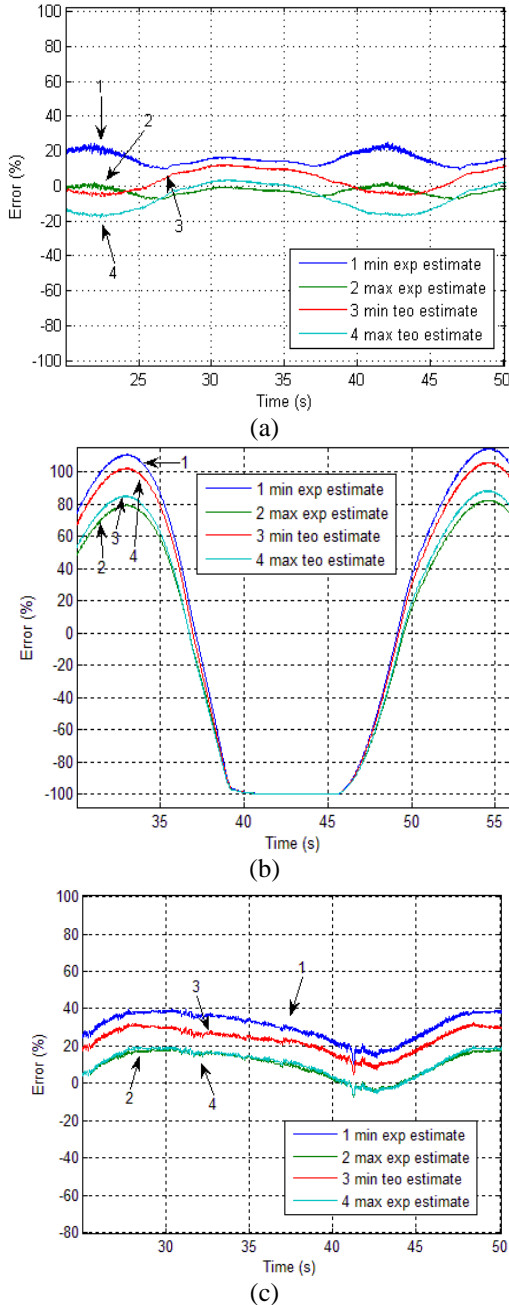


Figure 8: Current error for sinusoidal signals with amplitude of 1.74 mm and period of 20 s at  $p_s = 4 \text{ MPa}$   
 $T_s = 40^\circ\text{C}$ : (a) healthy valve (b) degraded valve (c) contaminated valve

Aiming to verify the effectiveness of the estimate model for fault detection three from twelve valve grooves were contaminated with diesel engine adhesive as shown in fig. 9.

This emulates the accumulation of dirt or varnish on the grooves. As can be seen in fig. 7b and fig. 8b, the valve did not lose its function and the controller was still able to be positioning the spool, even though it did it with increased error. However, the valve settling time was increased and the solenoid demanded more current yielding great differences between the estimates and the actual current even after the spool accelerating,. In fig. 8b one can notice the saturation of the solenoid current during the spool displacement. The error between actual and estimate current was greater than 100% during a considerable amount of time. Under these conditions a fault detection system would be able for fault detection and warning the operator before a valve jam occurred.

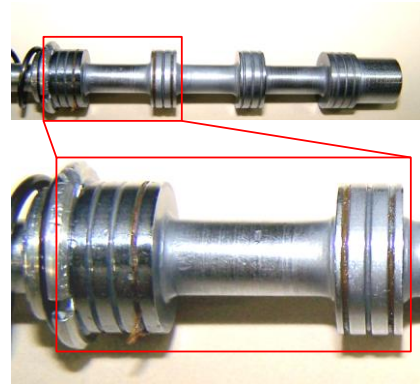


Figure 9: Valve with obstructed grooves

The spool valve without contaminants but with eroded control surfaces was also analyzed (fig. 10). The valve parameters such as the null spool position and the flow coefficients changed, and also the internal forces. As shown in fig. 7c, the current difference was higher than 20% even during steady state conditions. Figure 8c shows that with sinusoidal signals the error for the maximum estimate models (using theoretical or experimental parameters) was positive almost all the time indicating that the demanded current was greater than the estimated values indicating a potential fault. Even though with an eroded control surface the controller was still able to position the valve spool.

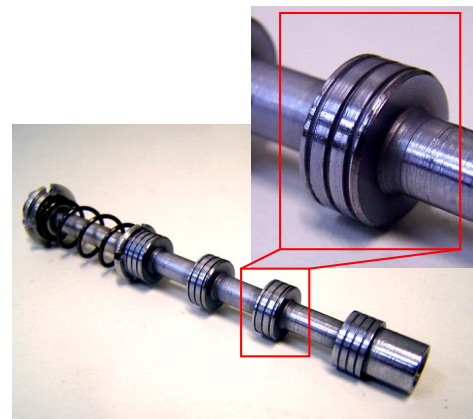


Figure 10: Valve with eroded control surfaces

## 4 Conclusions

The proposed model estimates adequately the solenoid current of a servo-proportional valve establishing minimum and maximum limits for an undamaged valve. Along with pressure measurement on valve ports and signals commonly available on the embedded electronic controller of servoproportional valves, an effective fault detection system can be designed using, for example, a simple rule based system. Although the model is based on steady-state equations, a difference between the actual and estimated current greater than the specified value taking into account the transient forces will be occurring when the valve is in poor conditions. Therefore, the model can be used for diagnosis under transient conditions as well, provided the estimates made during the initial spool acceleration are disregarded.

The sensibility of the system will depend upon the quality of the transducers, on the quality of the valve and on the user's tolerance to faults. If the transducers have a low uncertainty, the valve is linear and well balanced, the fluid is well filtered, and the application has little tolerance to changes in valve behavior, the user can set the system to warn after small errors between the estimates and the actual current are detected. However, if some of those conditions are not met, a higher error level should be tolerated before a fault is considered detected.

## Nomenclature

Designation	Denotation	Unit
$F_{fst}$	Steady-state flow force in axial direction	[N]
$\rho$	Fluid mass density	[kg/m <sup>3</sup> ]
$q_v$	Volumetric flow rate	[m <sup>3</sup> /s]
$A_0$	Metering orifice area	[m <sup>2</sup> ]
$\theta$	Jet angle at the <i>vena contracta</i>	[no dimension]
$cc$	Contraction coefficient	[no dimension].
$F_{fc}$	Reaction force on the spool	[N]
$x_c$	Valve spool displacement	[m]
$x_{cn}$	Nominal spool displacement	[m]
$K_v$	Valve flow coefficient	[m <sup>3</sup> /s.√Pa]
$p_1$	Inlet pressure	[Pa]
$p_2$	Outlet pressure	[Pa]
$A_{0n}$	Nominal metering orifice area	[m <sup>2</sup> ]

$cd$	Discharge coefficient	[no dimension]
$K_{esc}$	Valve spring rate due to $F_{fc}$	[N/m]
$F_c$	Force necessary to move the valve spool	[N]
$m_e$	Equivalent moving mass	[kg]
$B_e$	Equivalent viscous friction coefficient	[N.s/m]
$K_m$	Spring rate	[N/m]
$K_{me}$	Effective spring rate	[N/m]
$F_s$	Force produced by the solenoid	[N/m]
$K_{Fi}$	Solenoid force - current coefficient	[N/A]
$i_s$	Current on the solenoid	[A]
$b_s$	Solenoid force x current curve linear coefficient	[N]
$x_{c0}$	Spool null position	[m]
$x_{c\min}$	Minimum spool displacement for which the valve is linear	[m]
$x_{c\max}$	Maximum spool displacement	[m]
$x_{m0}$	Valve spring initial displacement	[m]
$a_i$	Angular coefficient of the current estimate model	[A/m]
$b_i$	Linear coefficient of the current estimate model	[A]
$\Delta p$	Valve pressure drop ( $p_1 - p_2$ )	[Pa]
$a_{a_i}$	Angular coefficient of $a_i$	[A/m.Pa]
$b_{a_i}$	Linear coefficient of $a_i$	[A/m]
$a_{b_i}$	Angular coefficient of $b_i$	[A/Pa]
$b_{b_i}$	Linear coefficient of $b_i$	[A]
$T_S$	Temperature at supply port	[°C]
$T_A$	Temperature at A port	[°C]
$T_B$	Temperature at B port	[°C]
$T_T$	Temperature at return port	[°C]

## References

- [1] International Organization for Standardization, 1998, "ISO 10770-1 Hydraulic fluid power - Electrically modulated hydraulic control valves – part 1: test methods for four way directional flow control valves", Switzerland.
- [2] Bhojkar, A., 2004, "Fault simulator for proportional solenoid valves". Thesis (Master of Science), Department of Mechanical Engineering of the University of Saskatchewan, Saskatoon, Canada. 115p.
- [3] Fenton, B., McGinnity, M., Maguire, L., September 2002, "Fault diagnosis of electronic systems using artificial intelligence". IEEE Instrumentation & Measurement Magazine, 1094-6969-02. pp. 16-20.
- [4] Bowers, M., Arnold, D. Crew, A. W., Gibson, R. J., Ghrist III, W. D., February 1989, "Diagnostic software and hardware for critical real-time systems", IEEE Transactions on Nuclear Science, Vol. 36, No.1. pp. 1291-1298.
- [5] Grimmeliuss, H. T., Meiler, P. P., Maas, H. L. M. M., Bonnier, B., Grevink, J. S., van Kuilenburg, R. F., April 1999, "Three state-of-the-art methods for condition monitoring", IEEE Transactions on Industrial Electronics, vol. 46, no. 2. pp. 407-416.
- [6] Parker Hannifin, 2005, "The handbook of hydraulic filtration", Metamora, USA. 38 p.
- [7] Vijlee, A., January 2003, "Roll-off cleanliness of hydraulic systems", Machinery Lubrication Magazine, no. 200301.
- [8] Park, R. W., August 1997, "Contamination control – a hydraulic OEM perspective", Workshop on Total Contamination Control Centre for Machine Condition Monitoring, Monash University. 18 p.
- [9] Merrit, H. E., 1967, "Hydraulic control systems", New York: John Wiley and Sons. 368p.
- [10] Tessman, R. K., Hong, I. T., 1998, "Contamination control of aircraft hydraulic systems", Stillwater: FES/BarDyne Technology Transfer Publication, no.10.
- [11] Doddannavar, R., Barnard, A., 2005, "Practical hydraulic systems: operating and troubleshooting for engineers and technicians". London: Elsevier. 232p.
- [12] Parker Hannifin, June 1999, "Tecnologia hidráulica industrial", M2001-1 BR, Jacareí, Brazil. 158 p.
- [13] ATOS Electrohydraulics, 2006, "KT Master catalog – KT06/E". Italy.
- [14] Atherton, B., 2007, "Discovering the root cause of varnish formation – the hidden issues beyond heat", Practicing Oil Analysis Magazine, Issue 200704, Noria Corporation, Tulsa, Oklahoma, EUA. pp. 22-25.
- [15] Fey, C., 1987, "Identifying Component Wear through Metallurgical Analysis", Proceedings of the 42<sup>nd</sup> National Conference on Fluid Power, Chicago, Illinois, USA, pp. 221-232.
- [16] Ramos Filho, J. R. B., 2009, "Análise teórico-experimental de falhas em válvulas direcionais servoproporcionais" Dissertation (Master in Mechanical Engineering) - Universidade Federal de Santa Catarina, Florianópolis, Brazil. 138 p.
- [17] Linsingen, I. v., 2003, "Fundamentos de sistemas hidráulicos" 2. ed., Florianópolis: Editora da UFSC. 399 p.
- [18] Stringer, J. D., 1976, "Hydraulic Systems Analysis", Macmillan. 192 p.
- [19] Johnson, J. L., "Design of Eletrohydraulic Systems for Industrial Motion Control". Parker Hannifin. USA, 1995.
- [20] Furst, F. L., 2001, "Sistematização do projeto preliminar de circuitos hidráulicos com controle de posição". Dissertation (Master in Mechanical Engineering) – Universidade Federal de Santa Catarina, Florianópolis, Brazil. 132 p.